GLOBAL SURVEY OF DUST DEVILS IN CTX DATA USING NEURAL NETWORKS. S. J. Conway[1] V. T. Bickel[2], M. R. Patel[3], L. Fenton[4] and H. Carson[5], [1] Nantes Université, Université d'Angers, Université du Mans, CNRS UMR 6112 Laboratoire de Planétologie et Géosciences, France (susan.conway@univ-nantes.fr). [2]ETH Zurich, Zurich, Switzerland. [3]School of Physical Sciences, Open University, Milton Keynes, UK. [4]Carl Sagan Center at the SETI Institute, Mountain View, CA, USA.[5]Department of Materials Science & Engineering, University of Washington, Seattle, WA, USA

Introduction: Dust devils are atmospheric vortices driven by daytime dry convective circulations and are visible because of the dust entrained from the ground [1]. They are common in deserts on Earth and globally on Mars. They appear as tubular or conical light-coloured clouds of dust that cast a dark shadow which is particularly distinctive in orbital images (Fig. 1). They migrate in the downwind direction and are often tilted as a result. They can reach much larger sizes on Mars (several km in height [2]), compared to Earth, perhaps because their size is limited by the depth of planetary boundary layer [3]. Here, we perform a global survey for dust devil vortices by using a neural network to search through the database of Context Camera (CTX) images aboard NASA's Mars Reconnaissance Orbiter spanning Mars Years 28-35.

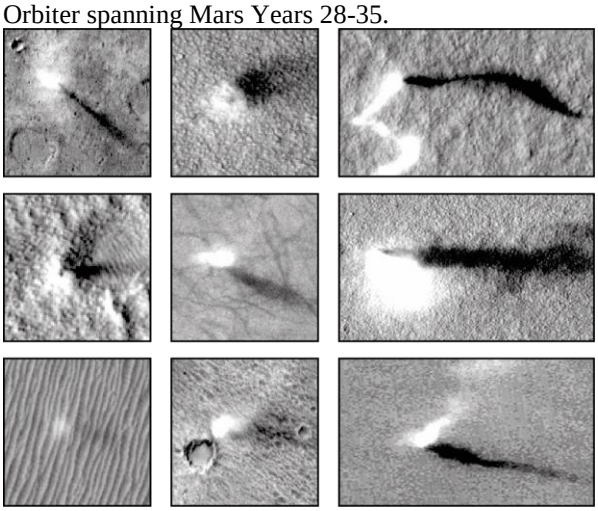

Fig. 1: Example dust devils detected in CTX images over different terrain types with a variety of shapes.

Approach: We used an off-the-shelf convolutional neural network (CNN) architecture (RetinaNet [4]) as used successfully for previous planetary studies [e.g. 5]. We trained two different neural networks, one for equatorial regions and one for polar regions, using data from a large variety of geographic locations taken from e.g. Fenton and Lorenz [3]. After training and testing (average precision AP ~0.7) we processed the whole database of CTX images (n=111,547 images) for dust devil detections using the JMARS-served CTX images [12]. We used one local (1x NVIDIA Titan Xp) and 4 Google Cloud Platform virtual machines (4x NVIDIA Tesla T4) to download and process the entire CTX image archive in ~6 weeks. Every detection with a CNN confidence level (CT) greater than 0.5 (n=57,051) was verified by a human operator. The bounding box output (which includes the bright core and most of the dark shadow as in Fig. 1) for each detection is loosely correlated with the dust devil's size. The effective diameter of the dust devil was estimated from the bounding box size by measuring the diameter of the "cloud" in a sample of 33 dust devils to generate a linear scaling relationship. We aim to improve this relationship by including more measurements in the near future.

Results: 3,747 images were found that contained validated dust devils at CT >0.5, comprising 11,201 individual detections. The images spanned MY 28 starting at Ls 114° through to MY 35 at Ls 114°. The median density of dust devils in this survey is 0.0004 km^{-2} (range 0.00009 to 0.2 km^{-2}), an order of magnitude lower than average densities found in the Amazonis monitoring area by Fenton and Lorenz [3]. Our effective diameters range up to 1.3 km and have a median of 251 m, but we need more calibration data before considering these absolute values reliable. However, we consider their relative sizes to be reliable, enabling comparison of dust devil dimensions between regions and seasons. Trends in frequency and size of dust devils with season agree with previous studies [3,6–8], where higher densities and larger sizes of dust devils are found in local summer for each hemisphere and low levels of activity occur in local winter (Fig. 2). The peak in size/density occurs just after the solstice in the southern hemisphere, but at the solstice in the northern hemisphere. Excluding known hotspots in Amazonis and Arcadia Planitiae we find that two broad latitudinal zones seem to exhibit both higher frequency and size: 55-70°N at Ls 120-150° and 50-70°S at Ls 300-330° (Fig. 3).

Conclusions: We present the most comprehensive temporal and spatial dust devil survey to date using a convolutional neural network on the full CTX image archive. Our findings generally agree with those from previous studies and in addition we highlight:

- A concentration of dust devils at latitudes around 60° in both hemispheres occurs around or just after

the respective summer solstices, which have above-average sizes, agreeing with observations of dust devil tracks [9].

- Valles Marineris and Elysium Planitia (InSight, MSL) are notable areas lacking dust devils despite good temporal image coverage.
- We confirm the hotspots of Chryse and Hellas Planitiae noted in some [9-11], but not all previous studies.
- We find two notable hemispherical asymmetries in the data: a) the peak in density and size is offset in time from the solstice in the southern hemisphere and not in the northern hemisphere, and b) the equatorial region follows the same temporal trends in size and density as the southern hemisphere. We attribute this to the dominance of the southern summer Hadley circulation [13] and are investigating this further using data from [14].

Acknowledgments: we thank the JMars team at ASU for hosting map projected CTX image products used in this work. SJC acknowledges the French Space Agency CNES for supporting her Mars work.

References: [1] M. Balme & R. Greeley (2006) *Rev. Geophys.*, *44*, RG3003. [2] L. Fenton *et al.* (2016) *Space Sci. Rev.*, *203*, 89–142.[3] L.K. Fenton & R. Lorenz (2015) *Icarus*, *260*, 246–262. [4] Lin *et al.* (2017) https://arxiv.org/abs/1708.02002 [5] V.T. Bickel *et al.* (2020) *Nat Comms*, 11, 2862. [6] B.A. Cantor *et al.* (2006) *JGR Planets*, *111*, 10.1029/2006JE002700. [7] M.R. Balme (2003) *JGR*, *108*, 5086. [8] J.A. Fisher *et al.* (2005) *JGR Planets*, *110*, 10.1029/2003JE002165. [9] P.L. Whelley & R. Greeley (2006) *JGR*, 111, E10003. [10] C. Stanzel *et al.* (2008) *Icarus*, 197, 39–51. [11] M.R. Balme (2003) *JGR*, 108, 5086. [12] P. R. Christensen et al. JMARS – A Planetary GIS, http://adsabs.harvard.edu/abs/2009AGUFMIN22A..06C [13] J.A. Holmes *et al.* (2020) *PSS*, 188, 104962. [14] M.I. Richardson and R.J. Wilson (2002) *Nature*, 416, 298.

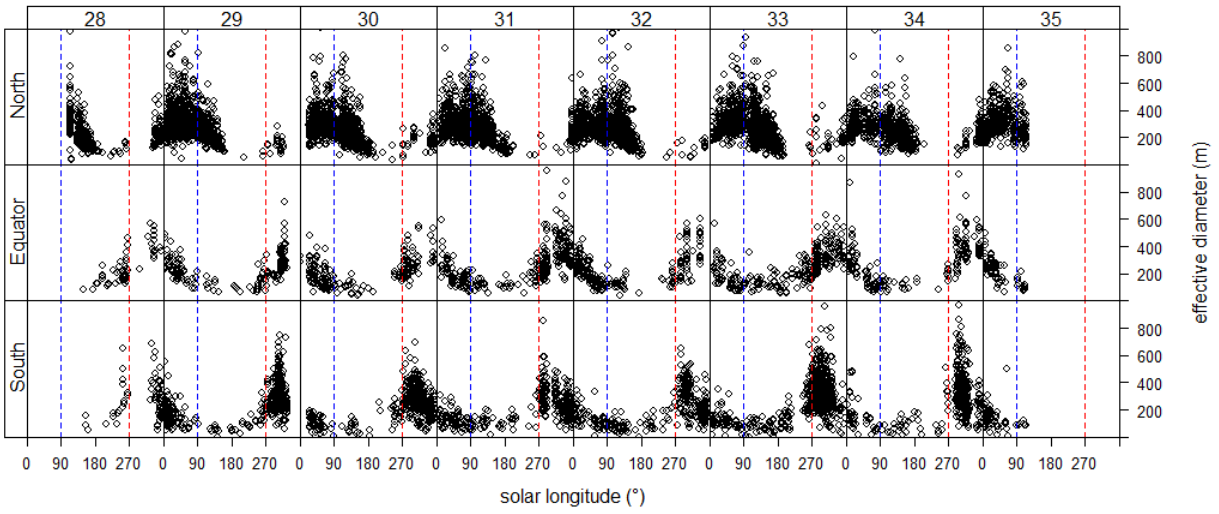

Fig. 2: Dust devil sizes with season (solar longitude) and Mars Year in the northern (>10°) and southern (<-10°) hemispheres and equatorial region (10°S-10°N). The blue dashed line is the northern summer solstice and red dashed line the southern summer solstice.

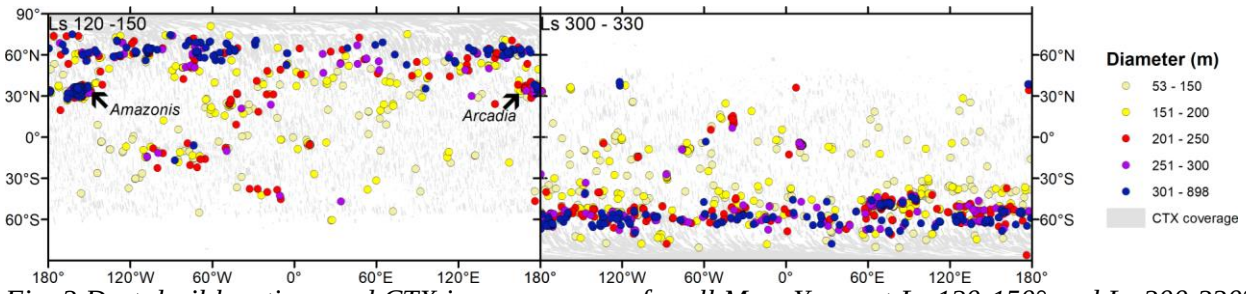

Fig. 3 Dust devil locations and CTX image coverage for all Mars Years at Ls 120-150° and Ls 300-330° showing concentrations of large dust devils around 60° latitude, north and south.